JOURNAL OF NEUROPHYSIOLOGY
Vol. 48, No. 6, December 1982. *Printed in U.S.A.*

Responses of Cortical Neurons to Stimulation of Corpus Callosum in Vitro

BRENT A. VOGT AND A. L. F. GORMAN

Departments of Anatomy and Physiology, Boston University School of Medicine, Boston, Massachusetts 02118

SUMMARY AND CONCLUSIONS

1. An in vitro slice preparation of rat cingulate cortex was used to analyze the responses of layer V neurons to electrical stimulation of the corpus callosum (CC). In addition, synaptic termination of callosal afferents with layer V neurons was evaluated electron microscopically to provide a structural basis for interpreting some of the observed response sequences.

2. Layer V neurons had a resting membrane potential (RMP) of 60 ± 0.68 (SE) mV, an input resistance of 47 ± 4.74 MΩ, a membrane time constant of 4.37 ± 0.51 ms, an electrotonic length constant of 1.38 ± 0.25, and produced spontaneous action potentials that were 50 ± 0.3 mV in amplitude. Intracellular depolarizing current pulses evoked spikes that were sometimes associated with low-amplitude (2–5 mV) depolarizing (5–10 ms in duration) and hyperpolarizing (10–20 ms in duration) afterpotentials.

3. A single stimulus of increasing intensities to the CC produced one of the following response sequences: *a*) antidromic spike and an excitatory postsynaptic potential (EPSP), which initiated one or more spikes; *b*) antidromic spike, EPSP-evoked action potentials, and a hyperpolarization, which may have represented an intrinsic cell property or inhibitory synaptic activity; *c*) EPSP and evoked spikes only; *d*) high-amplitude EPSP with an all-or-none burst of action potentials.

4. Antidromically activated (AA) neurons always produced EPSPs in response to CC stimulation. When compared with nonantidromically activated neurons, AA cells had a more negative RMP, greater electrotonic length constant (L_N), higher ratio of dendritic to somatic conductance (ρ), and formed shorter duration, callosal-evoked EPSPs.

5. Neurons in anterior cingulate cortex produced EPSPs of longer duration than did those in posterior cortex (50 ± 3.57 versus 26 ± 1.56 ms, respectively). EPSPs in anterior neurons also had a higher maximum amplitude (20.5 ± 1.0 versus 11.5 ± 0.79 mV) and longer time to peak (11.6 ± 2.2 versus 8.2 ± 0.8 ms).

6. Electron microscopy of Golgi-impregnated neurons following contralateral lesions demonstrated that both pyramidal and nonpyramidal neurons received direct callosal afferents. Synaptic termination of callosal axons with the apical dendritic trees of anterior pyramidal cells was 6 times greater than it was with posterior pyramidal neurons.

7. EPSP shape differences in anterior and posterior neurons may be partially accounted for by the density and distribution of callosal afferents to these two cortices.

INTRODUCTION

The slice preparation has proved to be a valuable tool for studying the membrane and synaptic response properties of mammalian neurons. This is particularly true of systems in which the neurons and afferent and intrinsic connections are segregated into discrete laminae such as in the hippocampus (23, 24, 35) and cerebellum (16, 36). Studies of neocortical areas in vitro (11, 26) have been limited to electrical stimulation of underlying white matter that contains a complex array of afferent axons from the thalamus, corpus callosum, and ipsilateral cortex. Responses produced by white matter stim-

0022-3077/82/0000-0000$01.25

ulation will necessarily be poorly defined due to the inability to restrict the stimulus to one afferent. However, we have been able to keep callosal axons and their termination sites intact in coronal slices of medial cingulate cortex in vitro for isolated stimulation of the corpus callosum (31). Antidromic and synaptic activity recorded in layer V neurons demonstrated the integrity of this pathway to its termination site.

Previous in vivo studies have described responses of neocortical neurons to electrical stimulation of contralateral cortex (3, 5, 14, 28). The responses differ greatly from those evoked by thalamic stimuli in that callosal-evoked responses have greater latency variability, EPSP amplitude variation, and an inhibitory postsynaptic potential (IPSP) may or may not be associated with the response. Although little is known about the structural basis for callosal-evoked responses, variations in EPSP time to peak in motor cortex neurons may be due to differences in afferent axon diameter and dendritic spine densities. Thus, slow-conducting pyramidal tract neurons have callosal-evoked EPSPs with slow rise times and have numerous dendritic spines, while fast-conducting pyramidal tract cells have an EPSP rise time 10 times faster than the slow-conducting cells and virtually no dendritic spines (13, 19). The present investigation presents an analysis of callosal-evoked responses in slices of cingulate cortex and proposes that EPSP shape variation may be accounted for by specific structural characteristics of this cortex.

METHODS

Slice preparation and maintenance

Male, hooded (Long-Evans) rats weighing 50–150 g were used for these experiments. Postwean rats (>21 days old) were employed because their brains were smaller and the callosal axons were more likely to be intact to their termination sites in 0.5-mm-thick slices. Neurons in animals of this age were developmentally mature in terms of the density of dendritic spines, number of primary basal dendrites, and somal volume (18). The rats were killed by decapitation and the brains were removed and placed in a cooled container (10–15°C). Lateral cortex was then removed with two parasagittal razor-blade cuts and the brain stem was removed with a rostrocaudal section through the septum and hippocampus (Fig. 1). Bilateral,

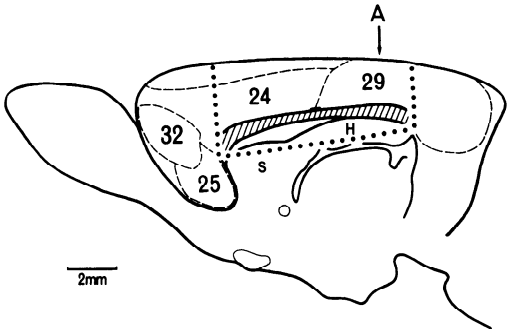

FIG. 1. Parasagittal section of the medial surface of the rat brain and topographic distribution of areas 25, 32, 24, and 29. The brain stem was removed with a rostrocaudal section through the septum (S) and hippocampus (H), and then bilateral, coronal slices were taken from anterior area 24 and posterior area 29 along the full length of the corpus callosum (hatched). The arrow at A indicates the level from which the slice in Fig. 2 was taken.

0.5-mm-thick coronal slices were cut from along the entire length of the corpus callosum (CC) and placed into a preincubation chamber that contained a low-calcium medium to reduce spontaneous synaptic activity. The preincubation medium was heated to 36°C, saturated with oxygen (95% O_2/5% CO_2), and contained the following (in mM): NaCl, 124; KCl, 5; KH_2PO_4, 1.24; $MgSO_4$, 1.3; $CaCl_2$, 0.8; $NaHCO_3$, 26; glucose, 10. Less than 7 min elapsed between decapitation and preincubation of the slices.

After about 40 min, slices were submerged in the recording chamber between a metal-mesh grid and a C clamp. The bathing medium flowed at a rate of 1–2 ml/min and contained a calcium concentration of 2.4 mM. The temperature of the medium was maintained at 36 ± 1°C by passing it through a Peltier device before it entered the recording chamber.

Stimulating and recording techniques

A pair of stimulating electrodes were positioned to straddle axons in the dorsal part of the CC (Fig. 2*B*). Stimulating electrodes were not placed directly in contralateral cingulate cortex, since that would have reduced the probability of stimulating axons that were intact to their termination sites. No afferents other than those from contralateral cortex are known to pass through this part of the CC. One electrode was steel and had a flat, bared tip that rested on top of the CC, while the second electrode was a pointed tungsten microelectrode that penetrated the CC. This electrode arrangement provided for maximal stimulation of callosal axons while producing minimal mechanical damage to it. Square pulses (0.1–0.2 ms in duration) were applied through these electrodes. Recording

electrodes were made from Omega dot glass capillary tubing, filled with 4 M potassium acetate, and connected to an electrometer with negative capacity feedback and an active bridge circuit, which allowed simultaneous measurement of voltage during the passage of current across the membrane. Electrode resistances measured 60–80 MΩ in the bathing medium. The bath ground was connected to a silver-silver chloride wire. Cellular responses were displayed and photographed on an oscilloscope and were also simultaneously recorded with a pen recorder.

Intracellular dye injections were made with electrodes filled with 3% lucifer yellow provided by W. Stewart. Following an injection, the slice was fixed for 4–8 h in phosphate-buffered 10% Formalin, sectioned into 100-μm-thick sections, mounted on chrome-alum-coated slides, and analyzed with a Zeiss epifluorescence microscope.

Electron microscopic techniques

Adult hooded rats (250–350 g) were used for analyzing the distribution of degenerating callosal afferents. The animals were anesthetized with Chloropent (0.32 ml/100 g body wt, Fort Dodge Laboratories, Fort Dodge, IA) and placed in a stereotaxic instrument. A longitudinal opening was made in the skull parallel to and 0.75–1.0 mm lateral to the midsagittal suture and extending from 2 mm anterior to bregma to 1 mm posterior to lambda. Then a scalpel blade, held parallel to the midline, was inserted 3–4 mm deep into the brain and drawn along the length of the cranial incision. Following a 3- to 4-day postoperative survival period, the animals were again anesthetized. During artificial respiration with 95% O_2/5% CO_2, the thorax was opened, 0.5 ml 1% sodium nitrite injected into the heart, and then 100 ml of fixative perfused through the heart. This first fixative contained 1% paraformaldehyde, 1.25% glutaraldehyde, and 0.015% calcium chloride in a 0.08 M cacodylate buffer at pH 7.2 and 30–40°C. This was followed by a similar volume of a second fixative, which contained 2% paraformaldehyde and 2% glutaraldehyde in a 0.08 M cacodylate buffer. The heads of these perfused animals were left in the refrigerator overnight and then the brains were removed and the contralateral cingulate gyri removed.

One of two rapid Golgi procedures were used to impregnate neurons; these procedures have been detailed in an earlier light microscopic analysis of neurons in cingulate cortex (32). Golgi-impregnated blocks were dehydrated in a graded series of glycerol in distilled water, superficially embedded in 7% agar, and cut into 100-μm-thick sections with a Sorvall tissue chopper. These sections were then surveyed light microscopically, and those containing impregnated neurons were rehydrated and gold toned with a 0.05% solution of gold chloride. The gold chloride was then reduced with oxalic acid and the original silver chromate precipitate removed with 1% sodium thiosulfate. The sections were then prepared for electron microscopy by poststaining with 2% osmic acid in 0.1 M cacodylate buffer at pH 7.2, dehydrated in a graded series of ethyl alcohol, en block stained with 1% uranyl acetate in 70% alcohol, and embedded in Epon-Araldite. Further details of this procedure have been reported elsewhere (7). The plastic-embedded, gold-toned neurons were drawn with a drawing tube attached to a Zeiss light microscope at a magnification of 1,250×. Thick (1 μm) sections were then cut and the relationship among blood vessels and impregnated neuronal processes drawn at a magnification of 250×. Finally, serial thin sections were cut, stained with lead citrate and uranyl acetate, and examined with an AEI-6 electron microscope.

It should be noted that strict quantification of this material is not possible (e.g., number of synaptic contacts formed by degenerating terminals with a unit length of dendrite). This is because all terminals do not degenerate at the same rate; early stages of terminal degeneration (e.g., vesicle clumping) are not convincingly degenerated and go uncounted, while at late stages of degeneration the spine head and its associated degenerating terminal may be pinched from the dendrite. Also, impregnation of spines and dendrites are often incomplete or the gold toning may have failed to precipitate on all previously silver-impregnated spines. In spite of these limitations, one can still make a rough estimate of whether apical dendrites form more synaptic contacts with callosal axons in anterior or posterior cingulate cortex by choosing similarly impregnated neurons from the same brain for comparison. Thus, lesion placement, postoperative survival time, and fixation are all constant, and the resulting observations represent the minimal number of actual contacts formed with each pair of neurons.

RESULTS

Cingulate cortex in vitro

The structure of posterior cingulate cortex is so well preserved in 0.5-mm-thick coronal slices (Fig. 2*A*) that fiber and cell dense layers can be visualized in the recording chamber with transillumination. The corpus callosum (CC) passing between the hemispheres can be seen as well as the white matter (i.e., cingulum) underlying cingulate cortex. Dense axonal plexuses occupy layers I and IV of area 29 of posterior cingulate cortex, while the light zone between these layers is packed

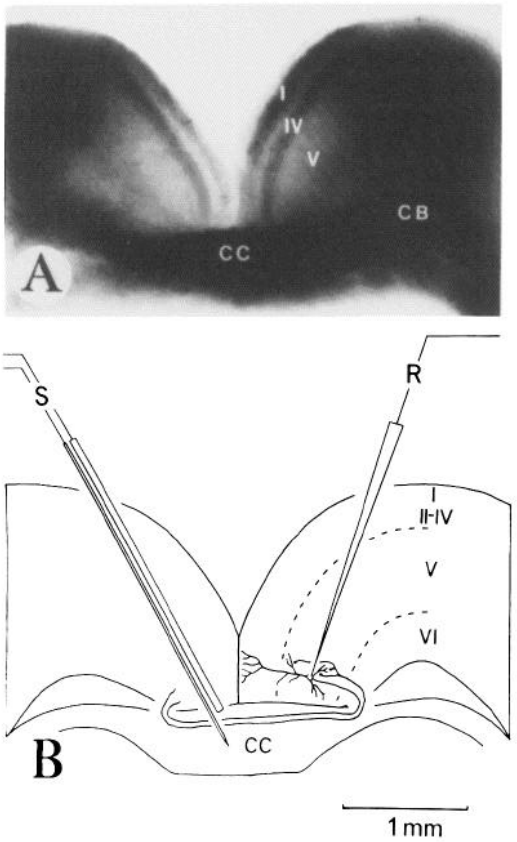

FIG. 2. Transillumination of posterior cingulate cortex (*A*) in which the corpus callosum (CC), cingulum bundle (CB), and layers I, IV, and V can be observed. *B*: bipolar stimulating electrodes (S) were placed in the CC in a contralateral position and the recording electrode (R) positioned in layer V.

with the somata of small and fusiform pyramidal neurons (32). Layer V is recognizable below layer IV, although the deeper border with layer VI is not very distinct. Finally, layers V and VI of area 29 receive most of the axonal terminals from contralateral cortex that originate from axons that pass through the CC (33).

The intracortical structure of area 24 in anterior cingulate cortex in vitro is less distinct than that of area 29, since the dense fiber plexuses are not present in the superficial layers of area 24. Location of the top of layer V, therefore, was made by measuring one-half the distance between the pia and white matter. Termination of callosal afferents in area 24 are distributed over a greater area than in area 29 such that most of the axonal terminals originating from contralateral area 24 are in layers I–III, with moderate numbers also present in layers V and VI (33).

Membrane properties of layer V neurons

Intracellular recordings were made in 61 neurons from layer V, of which 46 responded to electrical stimulation of the CC and 15 were not responsive to CC stimulation. Twenty-eight of the responsive cells were judged to be injured according to criteria previously established for hippocampal neurons (24) and reflected any combination of the following properties: low and/or unstable resting membrane potential (RMP), failure to discharge when depolarized with intracellular current, presence of synaptic-evoked action potentials without an underlying EPSP, and low-amplitude, broad action potentials. The typically "injured" cell had an RMP of less than 40 mV, would discharge only once to all depolarizing currents above threshold, and produced action potentials of less than 30 mV in amplitude.

Table 1 presents data collected from neurons that were both uninjured and responsive to CC stimulation ($n = 18$). The estimated RMP of these cells was 60 ± 0.68 (SE) mV with only one cell having an RMP below 50

TABLE 1. *Properties of layer V neurons*

	RMP, mV	τ_0, ms	τ_0/τ_1	L_N	EPSP Duration, ms	EPSP Amplitude, mV
Total	60 ± 0.68	4.37 ± 0.51	8.75 ± 1.32	1.38 ± 0.25	34 ± 1.29	14.7 ± 0.52
Anterior neurons	64 ± 2.4	4.29 ± 0.6	8.84 ± 1.57	1.24 ± 0.19	50 ± 3.57	20.5 ± 1.0
Posterior neurons	59 ± 0.91	4.48 ± 0.97	8.63 ± 2.52	1.55 ± 0.53	26 ± 1.56	11.5 ± 0.79

Values are means ± SE. EPSP duration and amplitude measured during maximal CC stimulation.

mV. Penetration discharge and spontaneous action potentials were 51 ± 0.3 mV in amplitude and were composed primarily of unitary spikes. Spontaneous discharges occasionally included doublets, but no spontaneous bursting was observed.

The input resistance (R_N) was determined from the slope of a current-voltage plot (Fig. 3*A*). The current-voltage plot was reasonably linear in the range tested and R_N for layer V neurons was 47 ± 4.74 MΩ.

The membrane time constant (τ_0) was estimated from voltage transients produced by 0.2-nA hyperpolarizing pulses (n = 9). Log (dV/dt) was determined from a series of tangent lines and plotted against time (Fig. 3*B*) and τ_0 was determined from the slope of a line fitted to the terminal exponential phase of this plot. An early, equalizing time constant (τ_1) was estimated by peeling the initial log (dV/dt) points (usually at $t \leq 1$ ms) from the line that was fitted to determine τ_0 (4, 12, 17, 21). The τ_0 for all layer V neurons was 4.37 ± 0.51 ms and τ_1 was 0.52 ± 0.05 ms; both were not significantly different for neurons located in either anterior or posterior cingulate cortex.

The time constant ratio (τ_0/τ_1) was used in two different equations to evaluate the electrotonic length (L_N) for these neurons. If the geometry of the neuron is reduced to an equivalent cylinder, L_N can be calculated from $\pi(\tau_0/\tau_1 - 1)^{-1/2}$ (21). An L_N value of 1.38 ± 0.25 was obtained for layer V neurons in cingulate cortex. A second method for estimating L_N incorporates the ratio of dendritic to somatic conductance (ρ). According to this procedure (10, 12) the point at which log ($\sqrt{T} \cdot dV/dt$) was maximum, when plotted against T, was first determined, where $T = t/\tau_0$ (Fig. 4*B*). T_{max} was then used to determine ρ from a theoretical plot of ρ versus T_{max} (10), producing a range of values of 0.8–8.0. Electrotonic length was then calculated

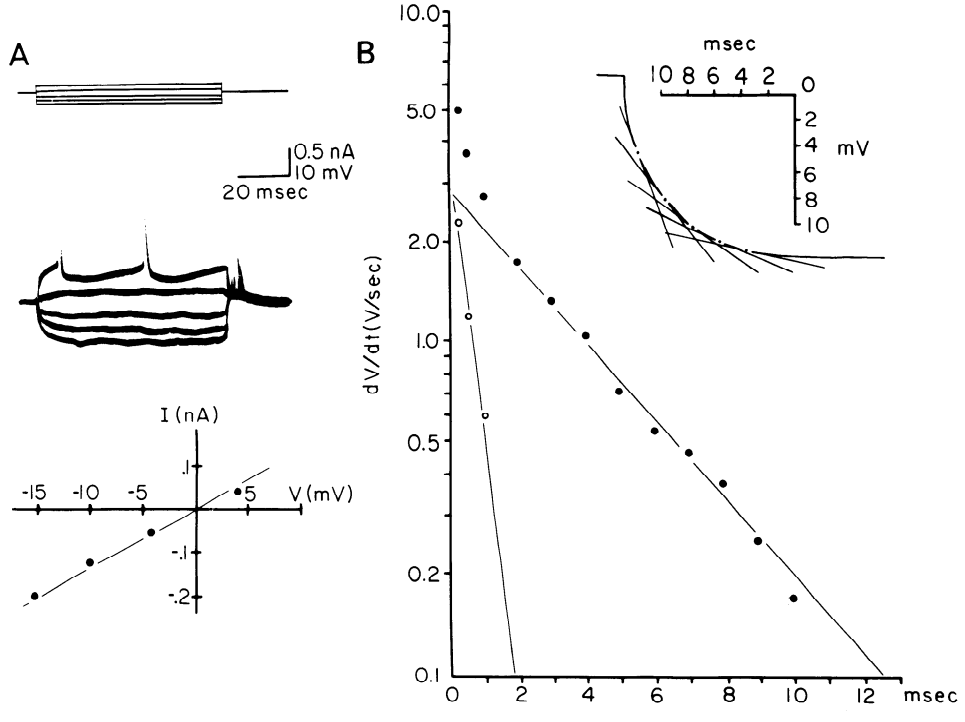

FIG. 3. Input resistance (R_N) and membrane time constant (τ_0) derived from voltage transients. *A*: voltage transients (middle trace) were produced by intracellular current pulses (top trace). The slope of the current-voltage plot for this cell indicated an R_N of 56 MΩ. *B*: a 0.2-nA hyperpolarizing pulse was used to determine the slope of the voltage (dV/dt) transient (inset, drawing of an actual response) and plotted semilogarithmically against time (ms). The slope of the line fitted to the terminal phase of this plot implied that τ_0 = 4.0 ms and a peeled early phase of τ_1 = 0.55 ms. Both *A* and *B* were from the same neuron.

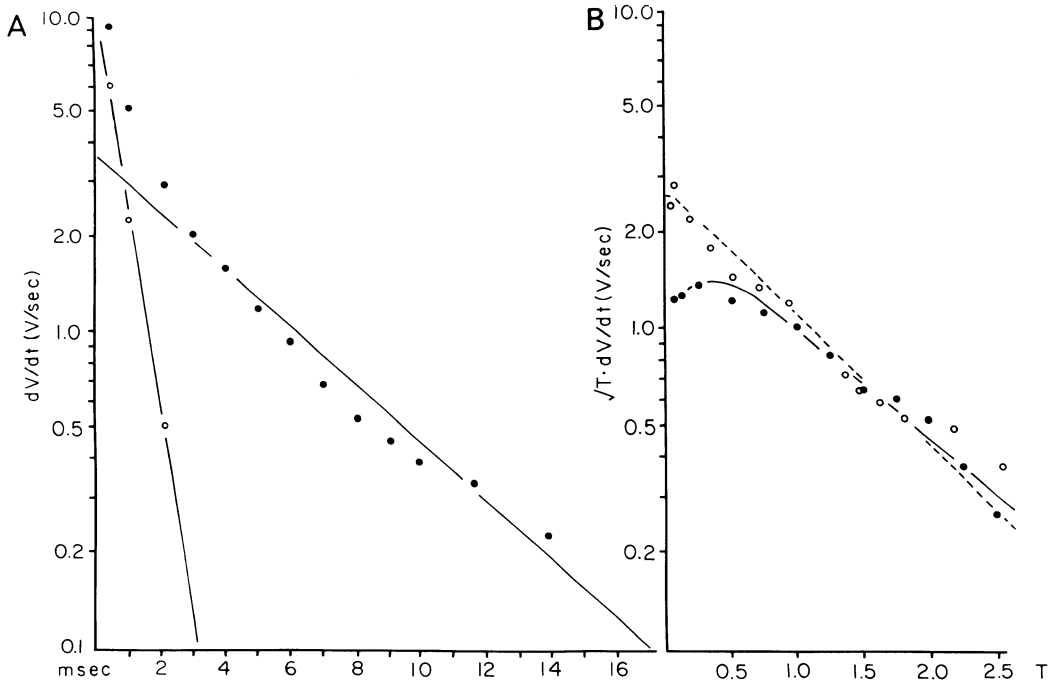

FIG. 4. Membrane time constant (3.4 ms) and equalizing time constant (0.8 ms) for a neuron that produced an antidromic action potential following CC stimulation (*A*). *B*: plot of $\sqrt{T} \cdot dV/dt$ against T, where $T = t/\tau_0$. T_{max} was 0.03 for the antidromically activated cell (dashed line) and it was 0.36 (solid line) for the cell in Fig. 3.

from this equation

$$L_N \simeq \pi \left(\frac{\rho/(\rho + 1)}{(\tau_0/\tau_1) - 1} \right)^{1/2}$$

Although T often reached its maximum too early to be determined, a value of 1.19 ± 0.22 was obtained for L_N when T_{max} was determinable.

Responses to electrical stimulation of corpus callosum

Responses to electrical stimulation of the CC included combinations of the following: antidromic action potentials, EPSPs, and associated synaptic-evoked spikes and low-amplitude hyperpolarizations. Antidromic action potentials were characterized by the absence of underlying EPSPs and were expected, since pyramidal neurons in layer V of cingulate cortex project axons across the corpus callosum (33). Antidromic spikes were 55 ± 1.4 mV in amplitude and had a duration of 0.44–1.1 ms when measured at half-maximum amplitude (Fig. 5*A*, *C*, *D*). Antidromic action-potential latencies ranged between 2 and 6 ms following CC stimulation, with a mean latency for six cells of 3.5 ms. Since the distance from stimulating electrodes to the recording site in layer V was approximately 1.6–2.0 mm, conduction velocities for antidromic spikes ranged between 0.33 to 0.8 m/s with a mean of 0.52 m/s.

EPSPs directly followed CC stimulation in neurons that did not produce antidromic spikes. With increasing stimulus intensities, these EPSPs summated and either evoked action potentials that each had distinguishable thresholds (Figs. 5*B* and 6*A*) or produced an all-or-none burst (Fig. 5*E*). In some instances depolarizing afterpotentials (DAPs) followed antidromic (Fig. 5*A*, *C*, and *D*) and synaptic-evoked (Figs. 5*A*, 5*B*, 6*A*, and 6*C*) spikes as in hippocampal neurons (34). The contribution of DAPs to spike initiation was probably limited, however, since they were only 2–4 mV in amplitude and 5–10 ms in duration when produced by spikes that were initiated with intracellular depolarizing current (Fig. 6*B*) or when they followed spontaneous action potentials. Stimulation of the CC when the membrane was depolarized to

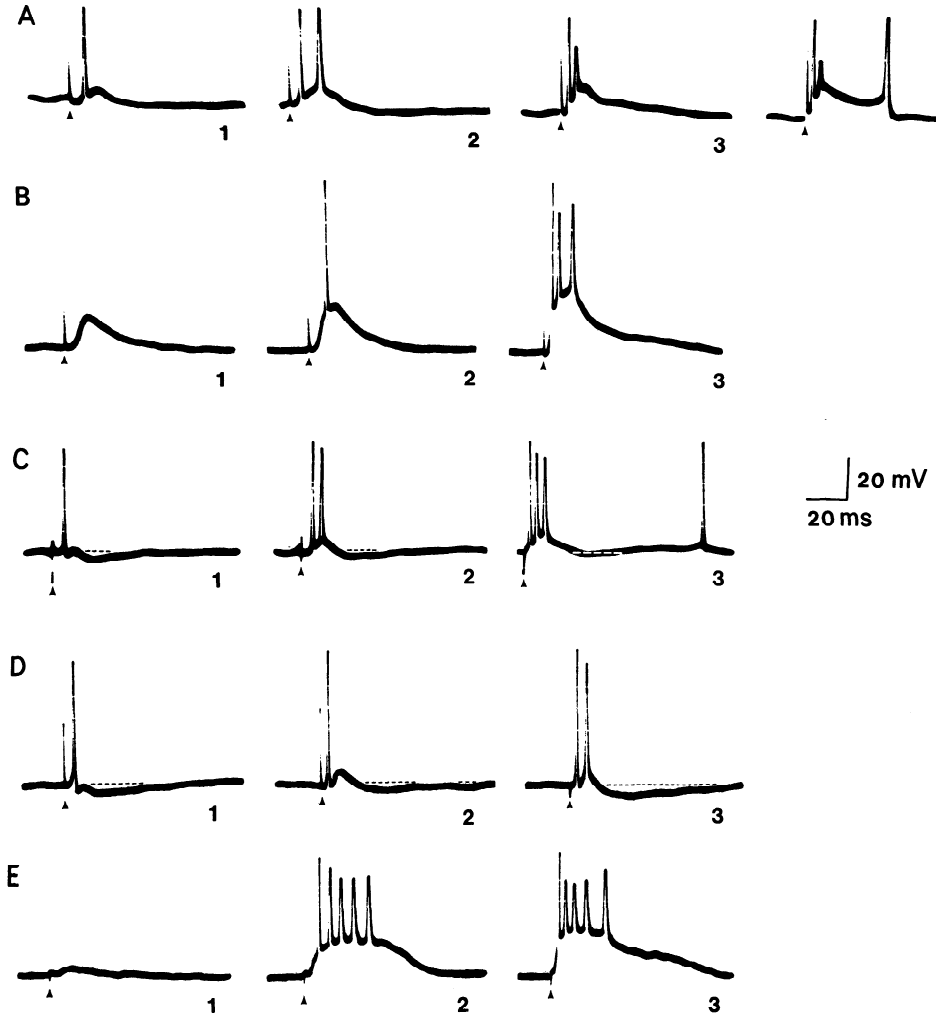

FIG. 5. Response sequences of layer V neurons to increasing intensities of electrical stimulation to the CC. *A*: antidromically activated spike and EPSP with evoked spikes that were partially inactivated at higher stimulation intensities, 3 and 4, anterior cingulate cortex. *B*: EPSP and evoked spikes, anterior cingulate cortex. *C*: antidromic spike, EPSP, and a hyperpolarization, which was suppressed with increased CC stimulation in posterior cortex, and *D*: in which the hyperpolarization was enhanced with increased CC stimulation. *E*: high-amplitude EPSP with an associated burst of action potentials. Arrowheads, stimulus artifact.

a potential similar to that which evoked a spike and DAP (Fig. 6*C*, −40 mV) resulted in a 14-mV afterpotential, of which approximately 11 mV was probably produced by excitatory synaptic activity.

All EPSPs decreased in amplitude when the membrane was depolarized and increased in amplitude when it was hyperpolarized (Fig. 6*C*). Plots of EPSP amplitude versus membrane potential (Fig. 6*D*) were linear in the tested ranges and the x intercept indicated a range of EPSP reversal potentials of 0 to −20 mV. EPSPs were also sensitive to high concentrations of magnesium in the bathing medium (>3 mM). Thus, a 5-min exposure of these cells to elevated magnesium reduced EPSP amplitude by 50% and the duration by 60%.

Variations in EPSP shape and the point of spike initiation resulted in three varieties of EPSPs (Fig. 7). First, low-amplitude (6–8 mV) monophasic EPSPs, which initiated action potentials directly at the peak of the EPSP and were followed by a hyperpolariza-

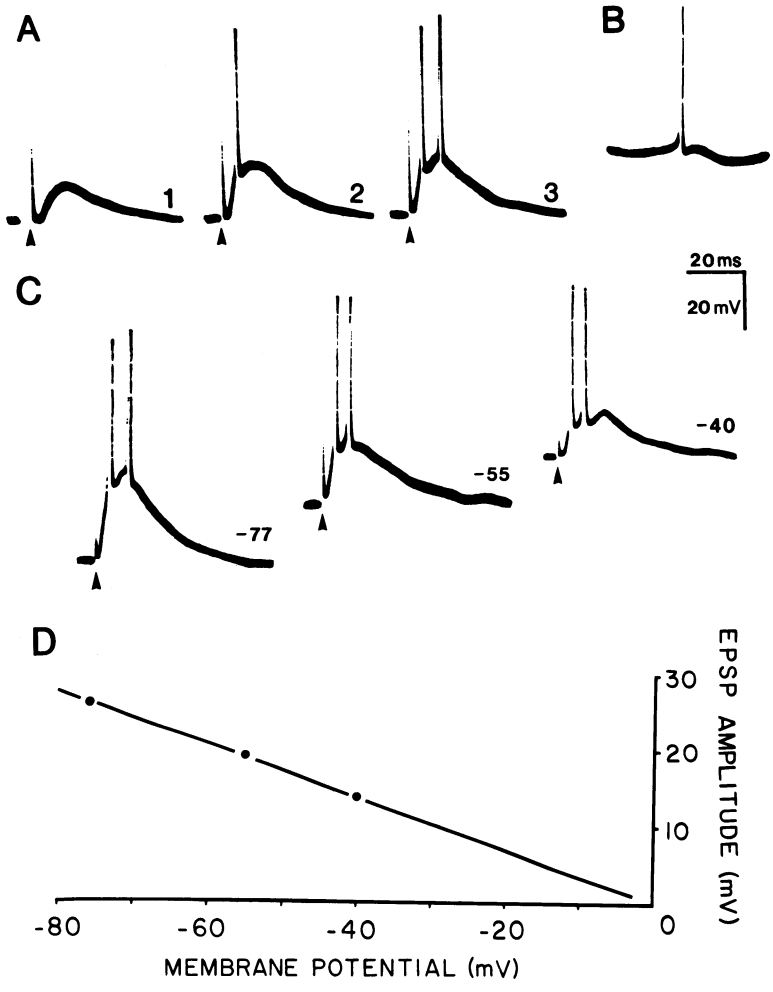

FIG. 6. EPSP amplitude variation at different membrane potentials. *A*: responses to increasing intensities of CC stimulation. *B*: membrane depolarization to −35 mV evoked action potentials, DAPs, and AHPs in this neuron. *C*: stimulation of the CC with the membrane hyperpolarized (−77 mV) depolarized (−40 mV) and at RMP (all CC stimulation intensities same amplitude). *D*: plot of maximum EPSP amplitude versus membrane potential indicated a reversal potential of 0 mV. Where action potentials distorted the response, a smooth curve was drawn through the trace to obtain an approximation of peak EPSP amplitude. Arrowheads, stimulus artifact.

tion. In some instances DAPs may have enhanced EPSPs and contributed to spike initiation. Second, higher amplitude (15–20 mV) EPSPs were seen, which had a rising phase of two different rates forming biphasic EPSPs, with spike initiation during the first phase. Although hyperpolarizing responses were not observed to follow these EPSPs, the faster decay during increased stimulation strengths may indicate the presence of an inhibitory effect. Third, low-amplitude (5–10 mV) and long-duration (50–90 ms) EPSPs were seen and, although they may have incorporated the unitary and/or biphasic forms, their long duration probably indicated different underlying transmitter action or afferent and intracortical circuitry.

Although hyperpolarizations that might be associated with inhibitory responses were not observed in neurons in layer V of anterior cingulate cortex following stimulation of the CC, 45% of the neurons in posterior cortex produced hyperpolarizing afterpotentials. Figure 5*C* indicates that weak CC stimulation evoked an antidromic spike, an EPSP that could initiate one action potential, and

a 20 ms duration, low-amplitude (4 mV) hyperpolarization. Stronger stimulation of the CC produced two synaptic-evoked spikes and the hyperpolarization was suppressed by the enhanced EPSP. Infrequently only one synaptic-evoked spike was produced and the hyperpolarization increased in amplitude with increased CC stimulation strengths (Fig. 5*D*). It was possible that these hyperpolarizations were the result of intrinsic membrane activity (34), since low-amplitude (2 mV) afterhyperpolarizations (AHPs) occasionally followed action potentials initiated by membrane depolarization (Fig. 6*B*) or followed spontaneous action potentials. It was also possible that some fraction of the hyperpolarization seen following callosal stimulation resulted from inhibitory synaptic activity, but further tests will be required to determine the exact contribution of this synaptic input.

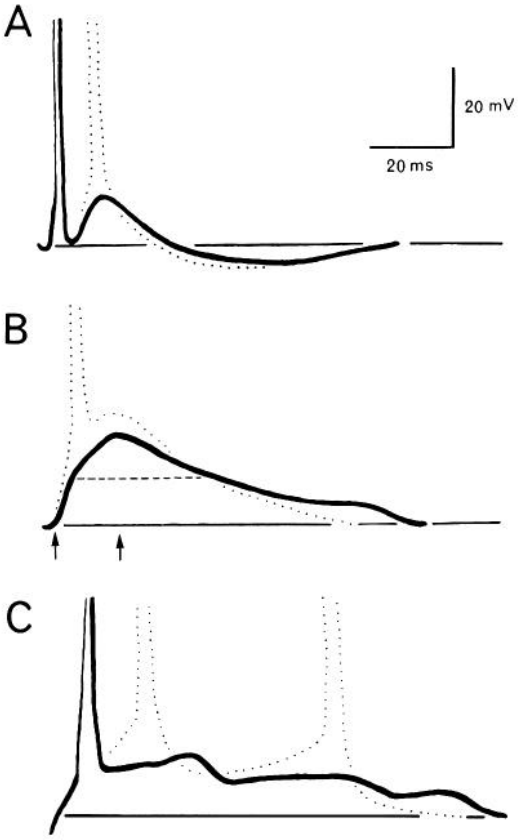

FIG. 7. Three EPSP shapes at low intensity (solid lines) and higher intensity (dotted lines) CC stimulation. *A*: low-amplitude, monophasic EPSP. *B*: higher amplitude, biphasic EPSP. Time to peak measurements were made from the point of EPSP inflection from RMP to peak EPSP amplitude (between arrows), while the half-width was the time for which the half-maximum EPSP was maintained (dashed line). *C*: low-amplitude, long-duration EPSP.

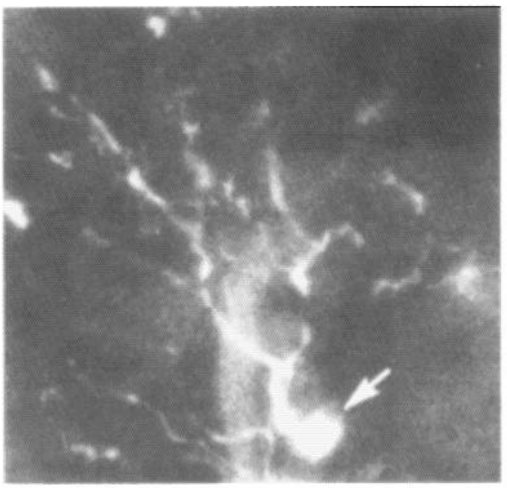

FIG. 8. Part of the dendritic tree of a lucifer yellow-injected multipolar cell. The soma was sectioned at the arrow. ×800.

Since layer V neurons that projected axons across the CC were mainly pyramids (33), it was of interest to compare the properties and responses of these antidromically activated (AA) with nonantidromically activated (NAA) neurons. NAA neurons may have been pyramids with axons that either did not pass through the CC or did so and the axon was not included in the slice. NAA neurons probably also included large multipolar neurons (32), since these cells were identified by injection with lucifer yellow (Fig. 8) and were observed to respond to CC stimulation. Some of these cells had axons that projected collaterals throughout layer III, which is characteristic of large multipolar neurons. AA neurons had more negative RMP than did NAA cells (−68 versus −55 mV, respectively) and higher L_N values (2.11 ± 0.57 versus 1.00 ± 0.04, respectively). ρ was also higher for AA than for NAA neurons (4.9 versus 0.85), indicating a larger dendritic-to-somatic conductance for pyramidal cells. AA neurons also had EPSPs that were of shorter duration (24 versus 40 ms) and lower amplitude (12 versus 17 mV). The lower am-

plitude EPSPs were partially accounted for by the fact that many neurons that had antidromic spikes also produced AHPs in response to CC stimulation, while only one NAA neuron had an AHP. Finally, the shorter duration EPSP of AA cells evoked only half the number of spikes as did the EPSPs of NAA cells (1.57 ± 0.48 versus 3.0 ± 0.45 spikes, respectively).

It can be seen in Table 1 that EPSPs evoked in anterior cortical cells were twice as long in duration as were those in posterior cells: 50 ± 3.57 versus 26 ± 1.56 ms, respectively. The amplitude of EPSPs in anterior cells were also almost twice as high as in posterior cells: 20 ± 1.0 versus 11.5 ± 0.79 mV, respectively. Since these means included a number of different types of EPSPs, a comparison of subthreshold, biphasic EPSPs was made using Rall's (20) EPSP time to peak and half-width measurements. Figure 7*B* indicates how these measurements were made: time to peak began at the point of EPSP deflection from RMP and continued to peak EPSP amplitude, while half-width was the duration of the EPSP at its half-maximum amplitude. Two anteriorally located neurons had a mean biphasic EPSP amplitude of 30.2 mV, time to peak of 9.5 ms, and a half-width of 19 ms, while two posterior neurons had a mean biphasic EPSP amplitude of 24.5 mV, time to peak of 6.2 ms, and a half-width of 16 ms. Thus, this subpopulation of EPSPs in anterior neurons were higher in amplitude, longer in duration, and reached peak amplitude more slowly than did those in posterior cortex. Comparison of time to peak for all EPSPs also showed that EPSPs of anterior neurons reached peak amplitude more slowly (11.6 ± 2.2 ms) than did those in posterior cells (8.2 ± 0.8 ms). It might have been expected that longer duration EPSPs in anterior neurons would result in a greater number of synaptic-evoked action potentials in anterior than in posterior cells. However, the maximum number of synaptic-evoked spikes (total number minus antidromically activated spikes) was only slightly greater in anterior than in posterior neurons (2.7 versus 2.3, respectively).

The higher amplitude and longer duration EPSPs of neurons in anterior cingulate cortex could have been accounted for in many ways: more negative RMP of anterior neurons, presence of hyperpolarizations in posterior cells, greater recurrent excitation in anterior cortex by antidromic activation, greater variation in conduction velocities for axons of anterior cells, greater multisynaptic excitation in anterior cortex, different transmitter and/or postsynaptic receptor properties, and/or greater numbers of callosal synapses formed with anterior neurons. Since the callosal and intracortical transmitters of these neurons are not known, these two options could not be assessed, while the others were partially addressed. First, although anterior neurons had slightly higher RMP than posterior cells (−64 ± 2.4 versus −59 ± 0.91 mV, respectively), it was unlikely that this difference accounted for EPSP amplitude differences, since there was an extremely low correlation between RMP and maximum EPSP amplitude (correlation coefficient, $r = 0.12$). Second, hyperpolarizing afterpotentials did reduce the maximum amplitude of EPSPs in posterior neurons but, if neurons that were hyperpolarized at any CC stimulation strength were removed from the sample, EPSPs in anterior neurons were still almost twice the amplitude of the remaining posterior cells. Thus, anterior cells had a maximum EPSP amplitude of 21 mV, while posterior neurons that did not produce an observable hyperpolarization had EPSPs of 13 mV in amplitude. Neurons in posterior cortex that responded to CC stimulation with a long-latency hyperpolarization had a maximum EPSP amplitude of only 9.4 mV. Third, recurrent excitation by antidromic activation was probably minimal in both cortices, since low-amplitude CC stimulation could be applied, which evoked only antidromic activity and failed to produce longer latency excitatory responses. It could not be determined whether high levels of CC stimulation resulted in antidromic excitatory responses. Fourth, it was unlikely that variation in callosal axon diameter could account for the 25 ms longer EPSP duration observed in anterior cells, since the latencies for all antidromic spikes only varied from 2 to 6 ms. Fifth, since there were significantly more synapses formed by callosal axons with anterior than with posterior pyramidal neurons, as described in the next section, this partic-

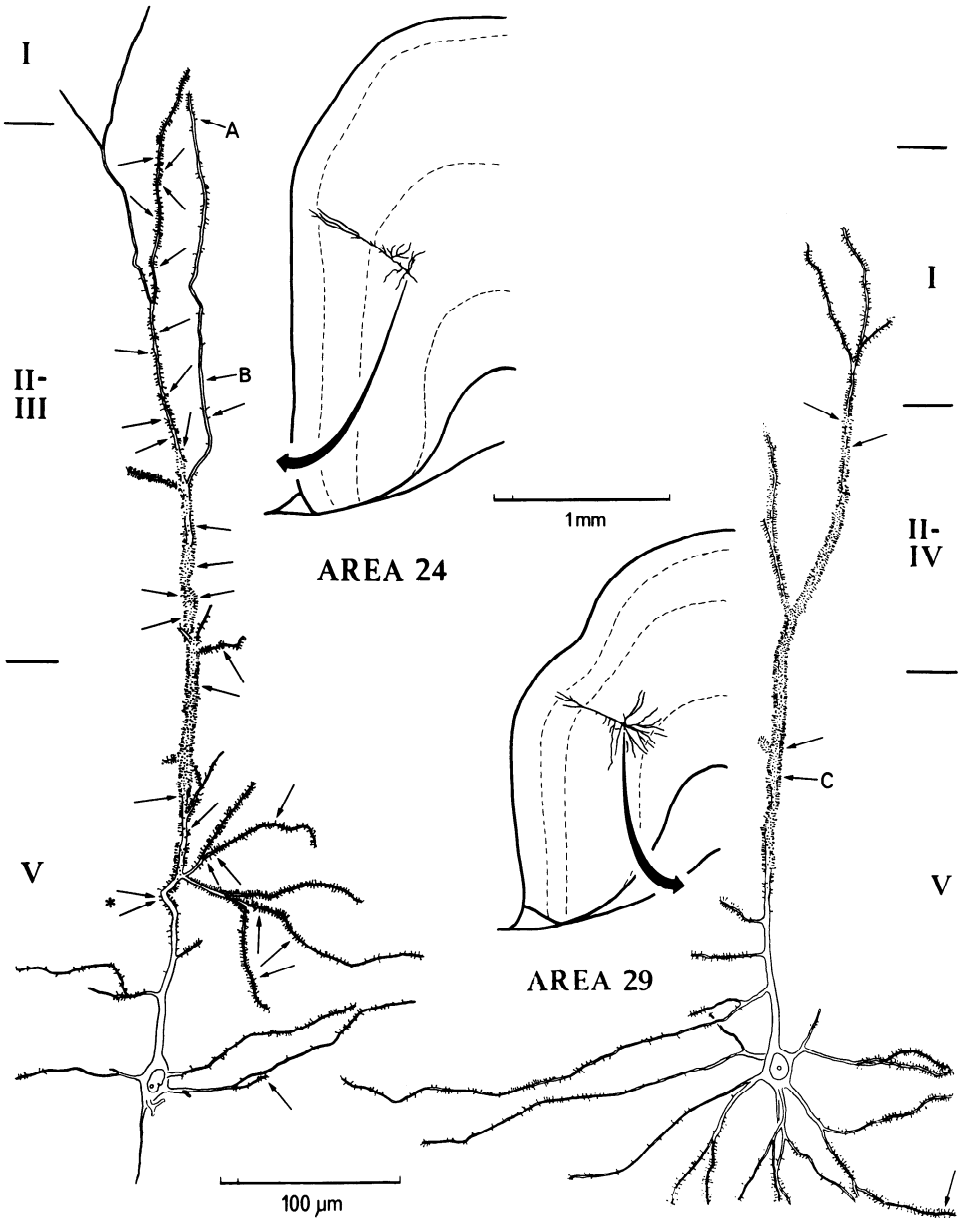

FIG. 9. A pair of layer V pyramidal neurons from anterior (area 24) and posterior (area 29) cingulate cortex. Insets are low-magnification drawings of the Golgi-impregnated neurons and their position in cingulate cortex (dashed lines are located at the top of layers II, V, and VI). Arrows at the high-magnification drawings point to places where degenerating callosal axon terminals formed asymmetric synapses with these neurons. The asterisk is a point where one terminal formed two synapses, while A, B, and C are places where synapses are presented in Fig. 10.

ular feature of anterior cingulate cortex may have accounted for the higher amplitude EPSPs.

Synaptic termination of callosal axons

The number of degenerated axon terminals in anterior cingulate cortex following a

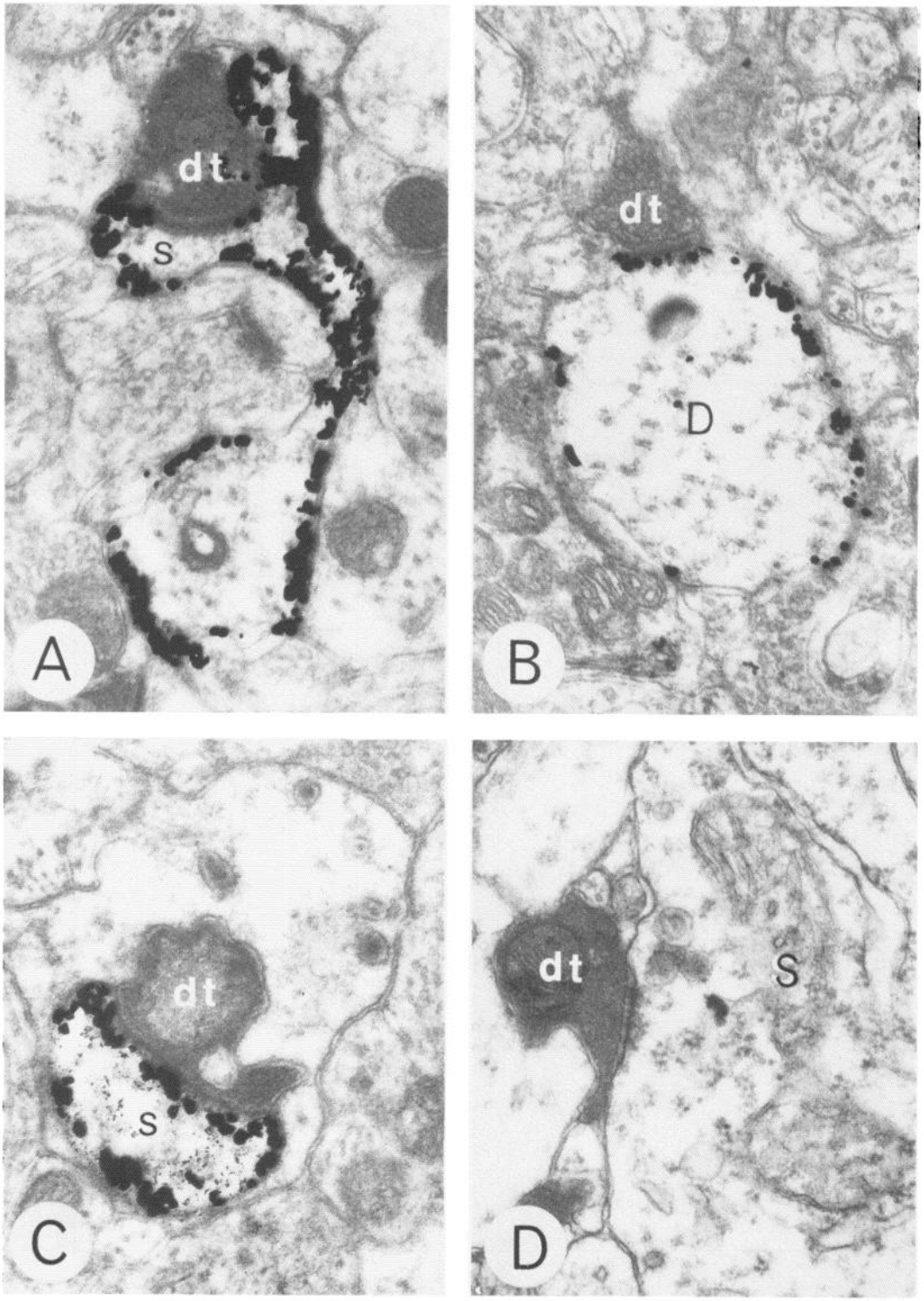

FIG. 10. Examples of synapses formed by degenerating callosal axon terminals. *A–C* were located at the levels indicated in Fig. 9. *A*: axospinous. *B*: axodendritic. *C*: axospinous. *D*: synapse formed with an unimpregnated nonpyramidal cell body. dt, degenerating axon terminal; s, spine head; D, dendrite; S, soma. ×25,000.

callosal lesion has been demonstrated to be approximately 5–6 times greater than in posterior cingulate cortex, and the terminals were found distributed throughout all layers in anterior cortex but were present mainly in layers V and VI of posterior cortex (33). The present analysis was undertaken to determine whether layer V pyramidal neurons received monosynaptic callosal afferents and whether the number and spacial distribution of synapses formed by callosal afferents with these pyramids reflected the overall number and laminar distribution just cited.

A survey of degenerating axon terminals indicated that most synapses formed by callosal afferents were asymmetric and with spines, while fewer were formed with smooth dendritic processes. Pyramidal neurons formed many synapses with degenerating callosal axon terminals. Comparison of callosal afferent termination with anterior and posterior neurons was made by evaluating layer V pyramidal neurons that had approximately the same-diameter somata and apical dendrites as well as a similar density of spines on the apical dendrites. Since posterior cortex was thinner than anterior cortex (0.6 versus 1.2 mm, respectively, between pia and white matter for plastic-embedded material), the length of the apical dendrites were consistently greater in anterior cortex.

Figure 9 presents drawings of two of the Golgi-impregnated pyramidal neurons, which were subsequently evaluated ultrastructurally. The pyramid in anterior cortex had a longer apical dendrite and passed through layers that contained a higher density of callosal terminals than did the pyramidal neuron from posterior cortex. Thirty-two synaptic contacts were formed by callosal terminals with the apical and basal dendrites of the anterior neuron (at arrows in Fig. 9), while only five synapses were formed with the apical and basal dendrites of the posterior neuron. Of the synapses formed with pyramidal cells, 95% were axospinous and 5% were axodendritic. Examples of these axospinous and axodendritic synapses are presented in Fig. 10. It may be possible to extrapolate the actual number of callosal synapses formed by these neurons according to a procedure presented in the DISCUSSION.

Although most degenerating terminals formed synapses with spines and smooth dendrites, an occasional asymmetric synapse was formed with a neuronal soma (Fig. 10*D*). Since the somata of pyramidal neurons did not form asymmetric synapses, it was concluded that these callosal synapses were formed with nonpyramidal neurons. The distribution of callosal terminals that form synapses with the dendrites of Golgi-impregnated nonpyramidal neurons has not been evaluated.

DISCUSSION

Afferent axons from contralateral cortex and their termination sites were preserved in bilateral, coronal slices of cingulate cortex. Layer V neurons responded to electrical stimulation of the corpus callosum much as cells of other cortices in vivo. Thus, antidromic spike conduction velocities ranged between 0.3 and 0.8 m/s, which was within the range reported for visual callosal axons in rabbit (0.3–12.9 m/s, Ref. 27). The primary response of neurons in cat motor and sensory cortices was excitatory (14, 28), with EPSP rise times of 1.3 and 14 ms for pyramidal tract neurons (19) compared to a range of 4–18 ms for cingulate neurons. The main differences with neocortical callosal-evoked responses were the higher amplitude EPSPs and limited IPSP activity of cingulate cells. Neocortical neurons had EPSPs that were less than 5 mV in amplitude, that evoked only one spike (5, 14) and these cells produced varying amounts of inhibition (3, 19, 28). There are two possible explanations for these findings: the extrinsic and/or intrinsic circuitry of cingulate cortex may differ from that of other cortical structures or preparation of the slice may alter connections that remain intact in vivo.

Since layer V pyramidal neurons in cingulate cortex project axons across the corpus callosum (33), it was reasonable to presume that antidromically activated (AA) neurons were pyramidal cells. Comparison of the membrane properties and responses of pyramidal and nonpyramidal neurons in the hippocampus with cingulate cells further suggests that AA neurons were pyramids and that nonantidromically activated (NAA) cells included nonpyramidal neurons. Hippocampal pyramids had a more negative RMP than

did interneurons (−70 versus −51 mV, respectively; Ref. 25), which was also true in cingulate cortex (−68 versus −55 mV, respectively), although this may reflect membrane injury. Hippocampal pyramids had a higher dendritic-to-somatic conductance ratio (ρ = 5 for pyramids versus ρ = 2.2; Ref. 29), which was the case for cingulate neurons (ρ = 5 for AA cells versus ρ = 0.9 for NAA cells). Also, electrotonic lengths of AA cells were greater than those for NAA cells in cingulate cortex (L_N = 2.11 versus 1.00, respectively). Finally, hippocampal interneurons produced bursts of action potentials to orthodromic activation, suggesting that excitation may have been greater in the perisomatic region (25, 29). In cingulate cortex, a greater number of spikes occurred in nonantidromic cells and asymmetric (i.e., excitatory) synapses were observed between callosal axon terminals and the somata of nonpyramidal cells. The major difference between hippocampal interneurons and cingulate cortex NAA cells was that hippocampal cells produced IPSPs in response to orthodromic stimulation, while only one NAA cell in cingulate cortex had a possible IPSP.

A consistent finding in the present analysis was the differences in callosal-evoked EPSP amplitudes and shape indices in anterior and posterior cingulate cortex. The higher amplitude and longer duration EPSPs that occurred in anterior neurons could have been accounted for by the passive membrane properties of these cells, the number and distribution of callosal synapses, and/or intrinsic, multisynaptic connections. Since the passive membrane properties (e.g., RMP, τ_0, L_N) of layer V AA and NAA neurons did not differ substantially in anterior and posterior cortices, it must be concluded that the callosal and intrinsic circuitry of cingulate cortex were responsible for differences in EPSP responses. Redman and Walmsey (22) have shown in cat spinal motoneurons that EPSP shape indices reflect anatomical differences in the distribution of afferent axons. Anatomical observations of the present analysis indicated that anterior cingulate cortical pyramidal neurons had longer apical dendrites and that some callosal synapses were formed at a greater distance from the somata than in posterior cortex. However, it was also found that as many as 6 times more synapses were formed with the dendrites of anterior than posterior pyramids. Increased EPSP amplitude due to activation of greater numbers of synapses would also influence the shape indices. In addition, while there is no direct evidence yet, it must be considered for long dendritic processes that there may have been active processes like voltage-dependent channels for the flow of inward and outward currents, which amplify the signal from dendritic regions and, therefore, alter the passive spread of the potential. Therefore, a strict interpretation of EPSP shape indices in terms of the electrotonic location of synapses would not be possible in cingulate cortex. Although the presence of DAPs, AHPs, and a variable, disynaptic inhibitory response also restricted the utility of these shape indices, it was generally true that CC stimulation activated more callosal synapses with anterior cortical neurons, thus lengthening time to peak and half-width measurements as well as increasing EPSP amplitude.

Studies of the distribution of callosal afferents on cortical pyramids using transneuronal degeneration techniques have suggested that these synapses were formed with the spines of oblique dendritic processes, while thalamic afferents terminated with spines of the primary apical dendrite (8, 9, 30). Although callosal synapses probably are formed primarily with apical dendrites, morphological observations of the present study indicated that callosal synapses are not segregated to any one apical dendritic compartment in anterior cingulate cortex. In contrast, posterior cingulate cortex receives most contralateral input in layers V and VI (33), and so it was not surprising that these pyramids received most callosal synapses on the proximal apical dendrites.

Although Golgi-degeneration procedures have limited quantitative value (see METHODS), it would still be of interest to estimate how many synapses are formed by callosal axon terminals with pyramidal neurons, since these synapses were activated during electrical stimulation of the CC in vitro. It was previously demonstrated that anterior cingulate cortex received as many as 6 times more callosal axon terminals than did posterior cingulate cortex (33). The present study extended this finding to show that the same proportion of synaptic contacts was made

directly with anterior and posterior pyramidal neurons. In Fig. 9, for example, there were 5 synapses formed with the posterior pyramid and 32 formed with the anterior cell, both of which were impregnated from the same brain. The anterior pyramid received most terminals in layers II and III, but the spines of branches of the apical dendrite were poorly impregnated such that some of the degenerated terminals in these layers that probably formed synapses with this neuron were missed (i.e., approximately six synapses, given the density of synapses formed with the well-impregnated dendrite). There were also a number of cut oblique branches on both cells, which may have resulted in an underestimate of as many as 20%, since this is the percentage of synapses that were formed with intact oblique dendrites. Thus, as many as 46 degenerating callosal synapses were probably formed with the anterior pyramid while 6 were probably formed with the posterior cell. Finally, comparison of electron microscopic degeneration and autoradiographic procedures has indicated that degeneration methods consistently underestimate by one-third the number of afferent synaptic contacts formed (6, 15). Therefore, the number of degenerating callosal synapses should be multiplied by 3, suggesting that the anterior pyramid probably formed at least 138 synapses with callosal axon terminals while the posterior neuron formed 18.

Figure 11 is a schematic summarization of some of the conclusions of this study. It is proposed that dendrites of pyramidal neurons receiving callosal afferents can be lumped electrically in an equivalent cylinder model

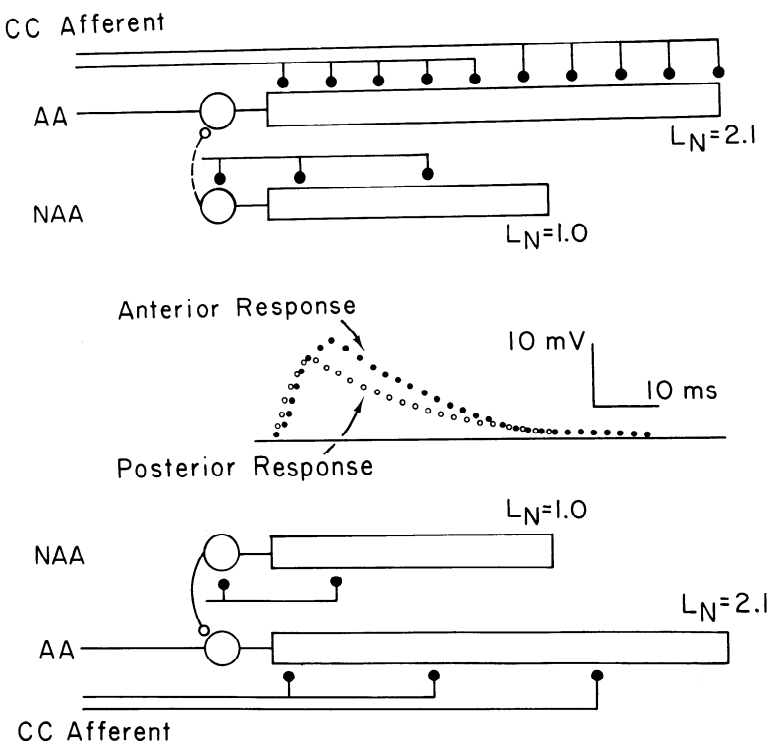

FIG. 11. Summary of some anatomical and electrical properties of layer V neurons. The CC afferent originates from many contralateral neurons and terminates widely as an excitatory (filled circles) current source. Antidromically activated (AA) neurons had a longer electrotonic length (L_N = 2.1) and a larger dendritic-to-somatic conductance ratio (ρ = 5) than did neurons that failed to produce antidromic spikes (NAA, L_N = 1.0, ρ = 0.9). Posterior NAA neurons are presented as having inhibitory (open circles), perisomatic connections with AA neurons, although small pyramids with different connections may also have been included in this sample. It is also possible that a similar inhibitory connection is present between anterior NAA and AA neurons (dashed line), although this has not yet been demonstrated. Responses are examples of averaged subthreshold, biphasic EPSPs that were not associated with overt IPSP activity.

of similar properties. Stimulation of the CC activates excitatory synapses in all dendritic compartments of anterior pyramidal cells (i.e., AA neurons) so that the callosal afferent system acts as a widely distributed current source, while fewer and more proximally located synapses would discharge posterior pyramidal cells. Although the NAA neuron category was probably a mixed population of pyramidal and multipolar cells, they are presented as an interneuron forming axosomatic synapses with AA neurons. This model provides a preliminary picture of the density and distribution of callosal synapses with cortical neurons, based on anatomical and electrophysiological data.

ACKNOWLEDGMENTS

We thank Drs. Carter Cornwall and Alan Peters for their many suggestions throughout the course of these studies and Dr. Anton Hermann for reading the manuscript.

This research was supported by National Institutes of Health Grants NS 11429 and NS 07016 and Boston University School of Medicine Award RR 05038.

A. L. F. Gorman died 12 July 1982.

Received 10 February 1982; accepted in final form 29 June 1982.

REFERENCES

1. ANDERSEN, P., ECCLES, J. C., AND LØYNING, Y. Pathway of postsynaptic inhibition in the hippocampus. *J. Neurophysiol.* 27: 608–619, 1964.
2. ANDERSEN, P. AND LØMO, T. Mode of activation of hippocampal pyramidal cells by excitatory synapses on dendrites. *Exp. Brain Res.* 2: 247–260, 1966.
3. ASANUMA, H. AND OKAMOTO, K. Unitary study on evoked activity of callosal neurons and its effect on pyramidal tract cell activity on cats. *Jpn. J. Physiol.* 9: 473–483, 1959.
4. BROWN, T. H., FRICKE, R. A., AND PERKEL, D. H. Passive electrical constants in three classes of hippocampal neurons. *J. Neurophysiol.* 46: 812–827, 1981.
5. CREUTZFELDT, O., MAEKAWA, K., AND HÖSLI, L. Forms of spontaneous and evoked postsynaptic potentials of cortical nerve cells. *Prog. Brain Res.* 31: 265–273, 1969.
6. DEKKER, J. J. AND KUYPERS, H. G. J. M. Quantitative EM study of projection terminals in the rat's AV thalamic nucleus. Autoradiographic and degeneration techniques compared. *Brain Res.* 117: 399–422, 1976.
7. FAIRÉN, A., PETERS, A., AND SALDANHA, J. A new procedure for examining Golgi impregnated neurons by light and electron microscopy. *J. Neurocytol.* 6: 311–337, 1977.
8. GLOBUS, A. AND SCHEIBEL, A. B. Synaptic loci on parietal cortical neurons: terminations of corpus callosum fibers. *Science* 156: 1127–1129, 1967.
9. GLOBUS, A. AND SCHEIBEL, A. B. Synaptic loci on visual cortical neurons of the rabbit: the specific afferent radiation. *Exp. Neurol.* 18: 116–131, 1967.
10. GORMAN, A. L. F. AND MIROLLI, M. The passive electrical properties of the membrane of a molluscan neuron. *J. Physiol. London* 227: 35–49, 1972.
11. GUTNICK, M. J. AND PRINCE, D. A. Dye coupling and possible electrotonic coupling in the guinea pig neocortical slice. *Science* 211: 67–70, 1981.
12. JOHNSTON, D. Passive cable properties of hippocampal CA3 pyramidal neurons. *Cell. Mol. Neurobiol.* 1: 41–55, 1981.
13. LABELLE, A. AND DESCHENES, M. Differential distribution of spines on the apical dendrites of slow and fast pyramidal tract cells in the cat. *Brain Res.* 164: 309–313, 1979.
14. LATIMER, L. N. AND KENNEDY, T. T. Cortical unit activity following transcallosal volleys. *J. Neurophysiol.* 24: 66–79, 1961.
15. LEVAY, S. AND GILBERT, C. D. Laminar patterns of geniculocortical projection in the cat. *Brain Res.* 113: 1–19, 1976.
16. LLINÁS, R. AND SUGIMORI, M. Electrophysiological properties of *in vitro* Purkinje cell somata in mammalian cerebellar slices. *J. Physiol. London* 305: 171–195 1980.
17. LUX, H. D., SCHUBERT, P., AND KREUTZBERG, G. W. Direct matching of morphological and electrophysiological data in cat spinal motoneurons. In: *Excitatory Synaptic Mechanisms*, edited by P. Andersen and J. Jansen. Oslo: Universitets Forlaget, 1970, p. 189–198.
18. MILLER, M. Maturation of rat visual cortex. I. A quantitative study of Golgi-impregnated pyramidal neurons. *J. Neurocytol.* 10: 859–878, 1981.
19. NAITO, H., NAKAMURA, K., KUROSAKI, T., AND TAMURA, Y. Precise location of fast and slow pyramidal tract cells in cat sensorimotor cortex. *Brain Res.* 14: 237–239, 1969.
20. RALL, W. Distinguishing theoretical synaptic potentials computed for different soma-dendritic distributions of synaptic input. *J. Neurophysiol.* 30: 1138–1168, 1967.
21. RALL, W. Time constants and electrotonic length of membrane cylinders and neurons. *Biophys. J.* 9: 1483–1508, 1969.
22. REDMAN, S. J. AND WALMSLEY, B. A. Combined electrophysiological and anatomical location of single group Ia fibre connexions with cat spinal motoneurones. *J. Physiol. London* 308: 99P–100P, 1980.
23. SCHWARTZKROIN, P. A. Characteristics of CA1 neurons recorded intracellularly in the hippocampal *in vitro* slice preparation. *Brain Res.* 85: 423–436, 1975.
24. SCHWARTZKROIN, P. A. Further characteristics of hippocampal CA1 cells *in vitro*. *Brain Res.* 128: 53–68, 1977.
25. SCHWARTZKROIN, P. A. AND MATHERS, L. H.

Physiological and morphological identification of a nonpyramidal hippocampal cell type. *Brain Res.* 157: 1–10, 1978.

26. SCHWARTZKROIN, P. A. AND PRINCE, D. A. Microphysiology of human cerebral cortex studied *in vitro*. *Brain Res.* 115: 497–500, 1976.
27. SWADLOW, H. A. AND WAXMAN, S. G. Variations in conduction velocity and excitability following single and multiple impulses of visual callosal axons in the rabbit. *Exp. Neurol.* 53: 128–150, 1976.
28. TOYAMA, K., MATSUNAMI, K., OHNO, T., AND TOKASHIKI, S. An intracellular study of neuronal organization in the visual cortex. *Exp. Brain Res.* 21: 45–66, 1974.
29. TURNER, D. A. AND SCHWARTZKROIN, P. A. Steady-state electrotonic analysis of intracellularly stained hippocampal neurons. *J. Neurophysiol.* 44: 184–199, 1980.
30. VALVERDE, F. Structural changes in the area striata of the mouse after enucleation. *Exp. Brain Res.* 5: 274–292, 1968.
31. VOGT, B. A. AND GORMAN, A. L. F. Response properties of layer V neurons to electrical stimulation of the corpus callosum in slices of cingulate cortex. *Soc. Neurosci. Abstr.* 11: 706, 1981.
32. VOGT, B. A. AND PETERS, A. Form and distribution of neurons in rat cingulate cortex: areas 32, 24 and 29. *J. Comp. Neurol.* 195: 603–625, 1981.
33. VOGT, B. A., ROSENE, D. L., AND PETERS, A. Synaptic termination of thalamic and callosal afferents in cingulate cortex of the rat. *J. Comp. Neurol.* 201: 265–283, 1981.
34. WONG, R. K. S. AND PRINCE, D. A. Afterpotential generation in hippocampal pyramidal cells. *J. Neurophysiol.* 45: 86–97, 1981.
35. YAMAMOTO, C. Activation of hippocampal neurons by mossy fiber stimulation in thin brain sections *in vitro*. *Exp. Brain Res.* 14: 423–435, 1972.
36. YAMAMOTO, C. Electrical activity observed *in vitro* in thin sections from guinea pig cerebellum. *Jpn. J. Physiol.* 24: 177–188, 1974.